Science of the Total Environment 835 (2022) 155546

Contents lists available at ScienceDirect

Science of the Total Environment

journal homepage: www.elsevier.com/locate/scitotenv

Community structure and function of epiphytic bacteria attached to three submerged macrophytes

Weicheng Yu [a], Jiahe Li [a], Xiaowen Ma [a], Tian Lv [a], Ligong Wang [a], Jiaru Li [b], Chunhua Liu [a,*]

[a] The National Field Station of Freshwater Ecosystem of Liangzi Lake, College of Life Science, Wuhan University, Wuhan, PR China
[b] College of Life Science, Wuhan University, Wuhan, PR China

HIGHLIGHTS

- Higher bacterial diversity was observed in epiphytic biofilm than surrounding water.
- Epiphytic bacterial diversity was higher during macrophyte decay than growth
- Epiphytic bacterial compositions and functions of *P. maackianus* were more abundant.

GRAPHICAL ABSTRACT

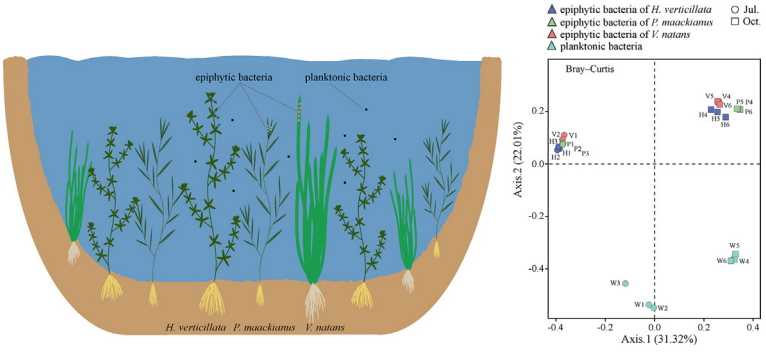

ARTICLE INFO

Editor: Abasiofiok Mark Ibekwe

Keywords:
Epiphytic bacteria
Functional traits
Planktonic bacteria
Growth season
Submerged macrophyte

ABSTRACT

In aquatic ecosystems, large amounts of epiphytic bacteria living on the leaf surfaces of submerged macrophytes play important roles in affecting plant growth and biogeochemical cycling. The restoration of different submerged macrophytes has been considered an effective measure to improve eutrophic lakes. However, the community ecology of epiphytic bacteria is far from well understood for different submerged macrophytes. In this study, we used quantitative PCR, 16S rRNA gene high-throughput sequencing and functional prediction analysis to explore the structure and function of epiphytic bacteria in an aquatic ecosystem recovered by three submerged macrophytes (*Hydrilla verticillata*, *Vallisneria natans* and *Potamogeton maackianus*) during two growth periods. The results showed that the community compositions and functions of epiphytic bacterial communities on the submerged macrophyte hosts were different from those of the planktonic bacterial communities in the surrounding water. The alpha diversity of the epiphytic bacterial community was significantly higher in October than in July, and the community compositions and functions differed significantly in July and October. Among the three submerged macrophytes, the structures and functions of the epiphytic bacterial community exhibited obvious differences, and some specific taxa were enriched on the biofilms of the three plants. The alpha diversity and the abundance of functions related to nitrogen and phosphorus transformation were higher in the epiphytic bacteria of *P. maackianus*. In summary, these results provide clues for understanding the distribution and formation mechanisms of epiphytic bacteria on submerged macrophyte leaves and their roles in freshwater ecosystems.

Abbreviations: WD, water depth; SD, secchi depth; Turb, turbidity; SS, suspended solids; WT, water temperature; pH, water pH; DO, dissolved oxygen; ORP, oxidation reduction potential; COD, chemical oxygen demand; Chl-a, chlorophyll *a*; TP, total phosphorus; TDP, total dissolved phosphorus; PP, particulate phosphorus; TN, total nitrogen; NH_4^+, ammonia nitrogen; NO_3^-, nitrate; DW, dry weight of biofilm; BChl-a, chlorophyll *a* content of biofilm; AI, autotrophic index; BTC, total carbon of biofilm; BTN, total nitrogen of biofilm; BTP, total phosphorus of biofilm.

* Correspondence author.
E-mail address: liuchh@163.com (C. Liu).

http://dx.doi.org/10.1016/j.scitotenv.2022.155546
Received 24 February 2022; Received in revised form 22 April 2022; Accepted 22 April 2022
Available online 27 April 2022

1. Introduction

Submerged macrophytes, as the main primary producers of shallow lakes, play important roles in the construction of lake community structures (Hilt et al., 2018), such as controlling sediment resuspension (Grace et al., 2019), adsorbing water suspended solids and facilitating nutrient uptake from the surrounding environment (Horppila and Nurminen, 2003; Wang et al., 2021b). Therefore, the restoration of submerged macrophytes is considered an effective measure to recover deteriorated and eutrophic lake ecosystems (Gao et al., 2017; Bai et al., 2020). In addition, the vast and favorable surfaces of leaves of submerged macrophytes can provide diverse habitats for bacteria (Schlechter et al., 2019; Wolters et al., 2019). Many previous studies have described these epiphytic bacteria on biofilms attached to submerged macrophytes (Yan et al., 2018; Zhao et al., 2019), which are thought to play important ecological roles in aquatic ecosystems (Coci et al., 2010; Srivastava et al., 2017; Ma et al., 2021). However, most previous studies have focused on the structure and function of epiphytic bacteria on submerged macrophytes in natural aquatic ecosystems (He et al., 2014; Xia et al., 2020). The community ecology of epiphytic bacteria during the ecological restoration of aquatic ecosystems is far from well understood.

Epiphytic bacteria may have complex interactions with planktonic bacteria (He et al., 2014). As epiphytic bacteria and planktonic bacteria cohabitate in the water, the two communities may exchange members (He et al., 2020; He et al., 2021). Previous studies have indicated that there are significant differences in the community compositions between epiphytic bacteria and planktonic bacteria (Burke et al., 2011; He et al., 2014). In contrast, some other studies claimed that the composition of epiphytic bacteria is very similar to planktonic bacteria and differs only at the genus or species level (Fan et al., 2016; Liu et al., 2019a). Therefore, the interactions between epiphytic bacteria and planktonic bacteria should be supported with more evidence.

Previous studies have revealed strong seasonal patterns for both epiphytic bacterial and planktonic bacterial communities (Salmaso et al., 2018). Both epiphytic bacteria and planktonic bacteria can be influenced by environmental factors, such as temperature, TP, and DO in water (Kuehn et al., 2014; Hao et al., 2017a). Moreover, in aquatic ecosystems, the presence of macrophytes could affect microbial communities by changing the horizontal and vertical heterogeneity of the aquatic environment (Wang et al., 2018; Xia et al., 2020). Therefore, with the growth of submerged macrophytes and the variations in environmental factors, the changes in the compositions and functions of epiphytic bacteria need further exploration.

Epiphytic bacteria may also have complex interactions with their host plants (Zhen et al., 2020; Wijewardene et al., 2022). Submerged macrophytes secrete and provide nutrients and oxygen to the attached bacterial communities, which is beneficial to their growth (Hempel et al., 2009; He et al., 2012). In return, epiphytic bacteria enhance elemental cycling and provide carbon dioxide to the macrophytes (He et al., 2014). Moreover, the different biofilm physicochemical properties of different plant species may result in host specificity of epiphytic bacteria (Gordon-Bradley et al., 2014; Fan et al., 2016). Different submerged macrophytes are usually used in the ecological restoration of lakes (Ge et al., 2018), and these different submerged plants have different leaf shapes. Whether there are significant differences in the biofilm and epiphytic bacterial community structure attached to the leaf surface of different submerged plants needs to be further studied.

In this study, we investigated epiphytic bacteria on three common submerged macrophytes as well as planktonic bacteria in two seasons during the process of submerged vegetation restoration in a shallow lake. We used quantitative real-time PCR and high-throughput 16S rRNA amplicon sequencing to analyze the bacterial community. We hypothesized that (1) higher diversity will be observed in epiphytic bacteria than planktonic bacteria, and both can be affected by season; (2) different submerged macrophyte species can differently affect the biofilm physicochemical properties and the structure and function of epiphytic bacteria.

2. Materials and methods

2.1. Study area and sampling

The study was performed in Jinhu Lake (30°26′24″ - 30°27′36″ N, 111°47′24″ - 111°50′02″ E), west of Hubei Province, China (Fig. 1). Jinhu Lake is located on the north bank of the middle reaches of the Yangtze River (Fig. 1). The catchment area is 4.98 km^2 with an average depth of 1.5 m and a maximum depth of 2.5 m. To improve the broken ecosystem of Jinhu Lake caused by intensive aquaculture, the local government stopped aquaculture and implemented a submerged macrophyte restoration project in 2018. After fish removal, the soaked fruits of *Vallisneria natans* and winter buds of *Hydrilla verticillata* were manually sowed in the lake while transplanting mature *Potamogeton maackianus* from January to May 2019. These three submerged macrophytes are common species in the middle and lower reaches of the Yangtze River and are often used in the restoration of eutrophic water (Chao et al., 2021; Li et al., 2021). Two years later, a relatively stable community dominated by three submerged macrophytes (*H. verticillata*, *V. natans* and *P. maackianus*) had formed in Jinhu Lake.

July is the middle growth period of the three submerged macrophytes in Jinhu Lake, while October is the late growth period. At the end of July and October 2021, the water and submerged macrophytes of three sites where the three macrophyte species cohabitated were sampled at a depth of 0.5 m. The sampling sites were spaced approximately 1 km apart and had similar hydrogeological and environmental conditions. For leaf samples, one sample was collected from the top (15 cm) of three to five plants of each species at each site. Approximately 10 g (fresh weight) of leaves were transferred to sterile 500 mL polyethylene bottles containing 400 mL of 50 mM phosphate-buffered saline (PBS, pH = 7.4) solution (Zhang et al., 2016; Xia et al., 2020) and subsequently underwent 3 min of ultrasonic treatment in an ultrasonic cleaner bath, 30 min in a shaker (225 r min^{-1}), and a further 3 min of ultrasonic treatment (Xian et al., 2020; Janssen et al., 2021). The suspension was then filtered through 0.22-μm membrane filters to collect epiphytic bacteria. Then, 150 mL of the suspension was filtered separately using a 0.45-μm filter to collect two biofilm filter samples for the determination of weight and chlorophyll *a* content. Moreover, enough leaves of each species were collected and then washed using distilled water and a soft brush to collect the eluent. The eluent was filtered through 250 mesh sieves first and then centrifuged at 4000 rpm for 15 min. The precipitate was air-dried, ground and passed through 100 mesh sieves to collect the biofilm for the determination of total carbon, total nitrogen and total phosphorus. Similarly, one water sample was collected at each site. Approximately 1 L of water was collected using an aseptic plastic bottle. Approximately 500 mL of water was filtered through 0.22-μm membrane filters to collect planktonic bacteria, and another 500 mL of water was used for chemical analyses. In total, 24 bacterial samples were collected and stored in a tank at −80 °C until DNA extraction.

2.2. Measurements of submerged macrophyte characteristics, water parameters and biofilm properties

Water temperature (WT), dissolved oxygen (DO), oxidation reduction potential (ORP), and pH of the water were measured using a YSI portable meter (YSI Incorporated, Ohio, USA). The secchi depth (SD) and water depth (WD) were measured with a black–white secchi disk and a handheld depth sounder, respectively. Turbidity (Turb) and total suspended solids (SS) were measured using a turbidity meter (2100Q, HACH, United States) and a portable spectrophotometer (DR900, HACH, United States). The above indicators were measured at the site at 10:00 a.m. The chemical oxygen demand (COD) was analyzed with the digestion solution for the corresponding parameters and landscape photometry (DR900, HACH, USA). The total nitrogen (TN), ammonia (NH_4^+), nitrate (NO_3^-), total phosphorus (TP), total dissolved phosphorus (TDP), particulate phosphorus (PP) and chlorophyll *a* (Chl-a) were measured according to the standard methods published by China's State Environmental Protection Administration. Moreover, submerged macrophyte samples were collected using a pronged grab sampler

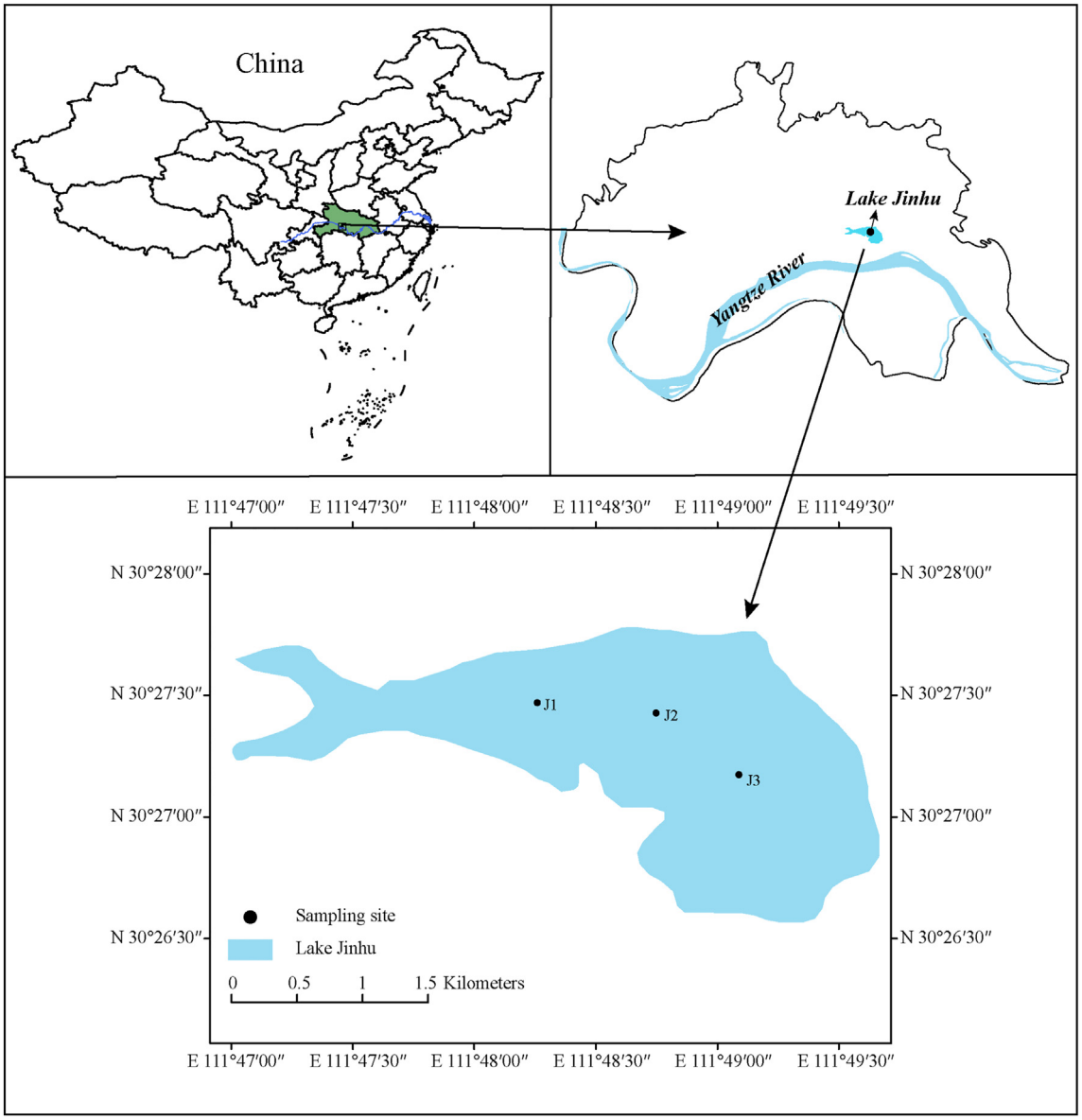

Fig. 1. Locations of the sampling sites in Lake Jinhu.

(25 cm × 35 cm) in each community. The collected submerged macrophytes were thoroughly cleaned and dried at 80 °C for 72 h to a constant mass. The total coverage of submerged macrophytes was determined by visual estimation, and the leaf area was measured by an area meter (LI-3100C, LI-COR, United States) (Lv et al., 2018). After the biofilm filters were weighed (fresh weight, FW), the filters were folded in half and placed in a crucible, dried at 105 °C to constant weight (dry weight, DW), placed in a muffle furnace, burned at 550 °C for 4 h, and then weighed (ash weight, AW) again to calculate the ash-free dry mass (AFDW) (Hamelin et al., 2015). The concentration of Chl-a in the biofilm was determined spectrophotometrically following 24 h of extraction in 90% acetone (Pei et al., 2015). The FW, DW, AW, AFDW and Chl-a were determined by the leaf area. The autotrophic index (AI) (Webb-Robertson et al., 2011) was calculated by determining the ratio of Chl-a to AFDW, which indicates the ratio of autotrophic to heterotrophic communities in the sample (Wu, 2016). The TC, TN and TP of the biofilm dry weight were analyzed according to standard methods (Bao, 2000).

2.3. Bacterial sequencing and PCR amplification

Total genomic DNA from samples was extracted using the CTAB method (Peng et al., 2019). DNA concentration and purity were monitored on 1% agarose gels. According to the concentration, DNA was diluted to 1 ng/μL using sterile water. 16S rRNA genes of distinct regions (16S V3-V4) were amplified using specific primers 341F (5′-CCTAYGGGRBGCASCAG-3′) and 806R (5′-GGACTACNNGGGTATCTAAT-3′) (Li et al., 2017) with barcodes. All PCRs were carried out with 15 μL of Phusion® High-Fidelity PCR Master Mix (New England Biolabs), 2 μM of forward and reverse primers, and approximately 10 ng of template DNA. Thermal cycling consisted of initial denaturation at 98 °C for 1 min, followed by 30 cycles of denaturation at 98 °C for 10 s, annealing at 50 °C for 30 s, and elongation at 72 °C for 30 s. Finally, the same volume of 1XTAE buffer was mixed with PCR products at 72 °C for 5 min, and electrophoresis was performed using 2% agarose gel for detection. PCR products were mixed in equidensity ratios. Then, the PCR products were purified with a Qiagen Gel Extraction Kit (Qiagen, Germany). Sequencing libraries were generated using the TruSeq® DNA PCR-Free Sample Preparation Kit (Illumina, USA) following the manufacturer's recommendations, and index codes were added. The library quality was assessed on the Qubit@ 2.0 Fluorometer (Thermo Scientific). Finally, the library was sequenced on an Illumina NovaSeq platform, and 250 bp paired-end reads were generated. The amplicon sequence variant (ASV) was obtained after quality control, denoising and the removal of chimeras using the DADA2 method

recommended by QIIME2 according to the raw sequence information (FASTQ format) (Callahan et al., 2016). The ASV was compared with the SILVA database and annotated (Reynaud et al., 2020). The ASV with 99% similarity was classified as one operational taxonomic unit (OTU) to obtain the OTU classification information table (Jiang et al., 2019). The OTUs were classified using the RDP classifier to obtain their numbers at different taxonomic levels.

2.4. Real-time quantitative PCR of the 16S rRNA gene

Real-time quantitative PCR was performed in triplicate to analyze the copy number of the 16S rRNA gene on an ABI 7500 Real-Time PCR System (Applied Biosystems, USA). The 16S rRNA gene was amplified using the primer pair 341F (5′-CCTAYGGGRBGCASCAG-3′) and 806R (5′-GGAC TACNNGGGTATCTAAT-3′) (Liu et al., 2019b). The 20 μL qPCR mixture contained 10 μL ChamQ SYBR Color qPCR Master Mix (Vazyme Biotech, Nanjing, China), 2 μL forward and reverse primers (5 μM), 1 μL template DNA and 7 μL sterilized ultrapure water. The specificity of the qPCR amplification was determined by performing melting curve analysis and gel electrophoresis. The PCR amplification was as follows: 95 °C for 5 min, followed by 40 cycles of 5 s at 95 °C, 30 s at 55 °C, and 40 s at 72 °C. To construct the qPCR plasmid, samples were amplified with primers, and the PCR products were purified by 2% agarose gel electrophoresis. The AxyPrep DNA Gel Extraction Kit (Axygen, Union City, CA, USA) was used to recover the target fragments. The fragments were ligated with the pMD18-T vector (Takara, Takara Bio Inc., Japan) and transferred to the *E. coli* strain, followed by blue–white screening to select the clonal strain. Standard curves for qPCR were constructed using 10-fold serial dilutions of the corresponding genes with plasmid DNAs of known concentrations. Gene abundances of each reaction were calculated based on the constructed standard curves ($R^2 = 0.9959$) and then converted to copies per gram of biofilm, assuming 100% DNA extraction efficiency.

2.5. Statistical analyses

A *t*-test was applied to test the differences in submerged macrophyte characteristics and water parameters between the two sampling periods. The differences in biofilm physicochemical properties, 16S rRNA gene abundances and microbial alpha diversity between different groups were analyzed by one-way ANOVA, followed by Tukey–Kramer post-hoc tests (Fahy et al., 2015). A Wilcoxon test (nonparametric method) was used to compare the dominant bacterial phyla and functions in the water and biofilm samples (Philonenko and Postovalov, 2015). The 'Venn diagram' package was generated to analyze the differences in planktonic bacteria and epiphytic bacteria between July and October, as well as the differences in epiphytic bacteria among the three different macrophytes (Chen and Boutros, 2011). A heatmap with hierarchical clustering based on the abundance table at the genus level was generated in the Complex Heatmap package in R software (Li et al., 2019). The beta diversity matrix was calculated using principal coordinate analysis (PCoA) and analysis of similarities (ANOSIM test) based on the Bray–Curtis distance using the 'vegan' package to detect the variations in plankton bacteria and epiphytic bacteria in different groups at the genus level (Chae and Warde, 2006; Liu and Tong, 2017). To identify different microbial species among the different groups, we used linear discriminant analysis effect size (LEfSe) analysis based on linear discriminant analysis (LDA). We assessed the significant differences, with an LDA score > 3.5 as the critical value (Kozik et al., 2017). To analyze microbial energy metabolism functions, PICRUSt2 was used to predict the microbial function based on the 16S rRNA sequence information and KEGG function information (Douglas et al., 2020). All the above analyses were conducted in R 3.5.1.

3. Results

The biomass and coverage of submerged plants, Turb, WT, pH, TP, TDP, PP, TN and NH_4^+ in water were significantly higher ($P < 0.05$) in July than

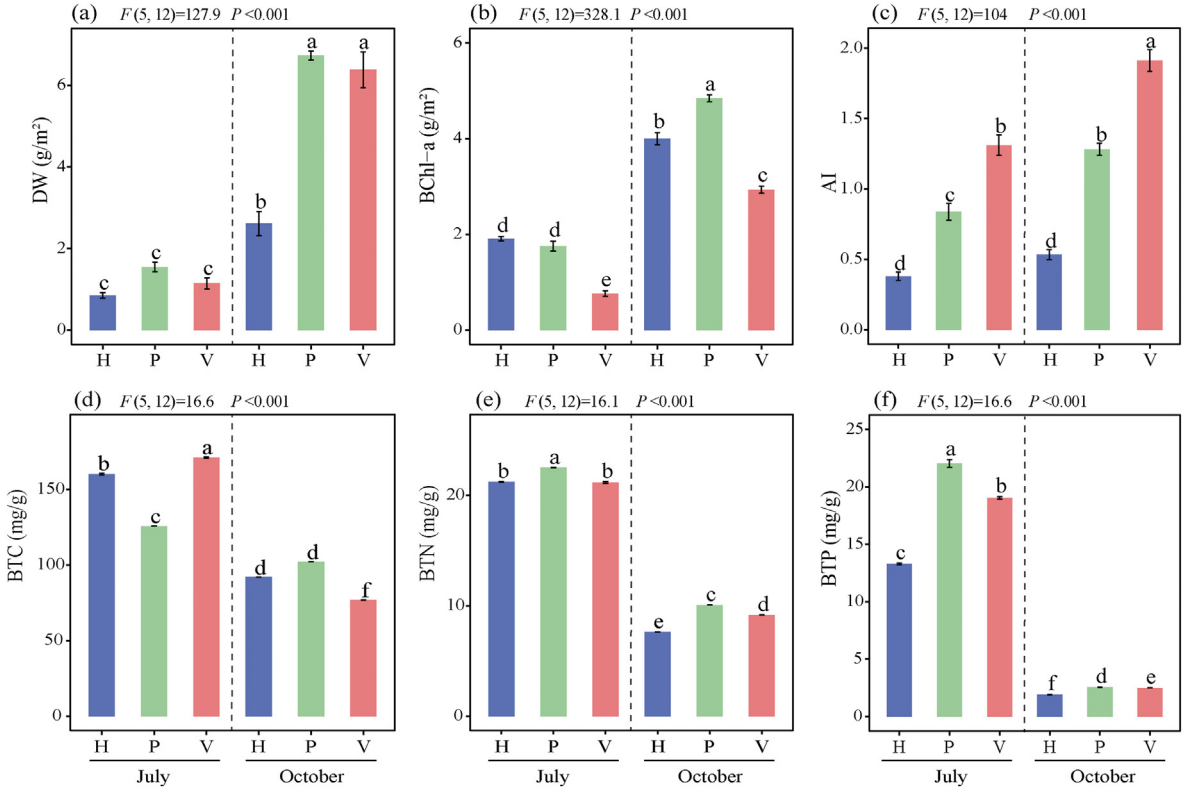

Fig. 2. Physicochemical properties of biofilms on three submerged macrophytes in July and October: (a) DW, dry weight; (b) BChl-a, chlorophyll *a* content of the attached biofilm; (c) AI, autotrophic index; (d) BTC, total carbon of biofilms; (e) BTN, total nitrogen of biofilms; (f) BTP, total phosphorus of biofilms. H, biofilm of *H. verticillata*; P, biofilm of *P. maackianus*; V, biofilm of *V. natans*. Different letters represent significant differences ($P < 0.05$) in mean value by means of one-way ANOVAs and LSD post-hoc comparisons.

in October (Fig. S1a, b, e, g, h, m-q); however, the SD, DO, COD and Chl-a were significantly higher in October than in July (Fig. S1d, i, k, l). July and October had similar values of WD, SS, ORP and NO_3^- in water (Fig. S1c, f, j, r).

3.1. Biofilm physicochemical properties

The DW, Bchl-a, and AI of biofilms attached to the three different submerged macrophytes were significantly higher in July than in October (Fig. 2a-c); however, the opposite patterns were found in the BTC, BTN and BTP of biofilms (Fig. 2d-f). Except for a lower DW of biofilms found in *H. verticillata* in October, a similar DW of biofilms was found in the three species (Fig. 2a). The Bchl-a of *V. natans* was lower than that of *H. verticillata* and *P. maackianus*, while the AI was higher than that of *H. verticillata* and *P. maackianus* (Fig. 2b, c). Except for the lower BTC in July, the BTC, BTN and BTP of *P. maackianus* were all the highest in the three submerged macrophytes (Fig. 2d-f).

3.2. Abundances and alpha diversity of epiphytic bacteria and planktonic bacteria

In total, 2,279,662 available raw readings were obtained from all 24 samples, with an average reading of 94,986 ± 8511 per sample. After quality control and rarefication, 1,761,149 unique representative sequences were generated, and the total number of OTUs was 14,470. The rarefaction curves constructed from the sequenced data were stable, indicating that the sequencing depth was sufficient to study the microbiota (Fig. S2). The 16S rRNA gene abundance of bacterioplankton was significantly higher ($P < 0.05$) in October than in July (Fig. S3a). In July, the highest abundance of epiphytic bacteria occurred on *H. verticillata* leaves, and the lowest occurred on *V. natans*; however, the tendency was reversed in October (Fig. S3b). Except for the Shannon index of *H. verticillata* and Pielou index of *V. natans* in July, the alpha diversity of epiphytic bacteria was significantly higher than that of bacterioplankton (Fig. 3). The alpha diversity of both bacterioplankton and epiphytic bacteria was significantly higher in October than in July (Fig. 3). Among the three submerged macrophytes, the highest alpha diversity of the epiphytic bacteria was found on *P. maackianus* leaves (Fig. 3).

3.3. Community composition of epiphytic bacteria and planktonic bacteria

Based on comparisons with the Silva bacterial database, 44 microbial phyla were detected in all samples, comprising 102 classes, 247 orders, 422 families, and 954 genera. The dominant epiphytic bacterial phyla present in the biofilms attached to submerged macrophyte leaves, ranked in decreasing order by mean relative abundance, were *Proteobacteria*, *Cyanobacteria* and *Bacteroidetes*; similarly, the dominant bacterioplankton phyla were *Proteobacteria*, *Bacteroidetes*, *Cyanobacteria* and *Actinobacteria* (Fig. 4a). Based on the OTUs, Venn diagrams were drawn to calculate the unique and common features of the epiphytic bacteria in the three submerged macrophytes (Fig. 4b) as well as the epiphytic bacteria and planktonic bacteria in July and October (Fig. 4c). At the phylum level, the abundance of *Proteobacteria* and *Cyanobacteria* was significantly higher ($P < 0.05$) in epiphytic bacteria than in bacterioplankton, while *Actinobacteria* showed the opposite pattern (Fig. S4a). Among epiphytic bacteria, the phylum *Proteobacteria* was significantly more abundant in October than in July ($P < 0.01$), while *Cyanobacteria* showed the opposite pattern (Fig. S4b). Regarding the abundance of bacterioplankton, the phyla *Actinobacteria* and *Chloroflexi* were significantly more abundant in October than in July (Fig. S4c). Compared with *H. verticillata*, the phyla *Armatimonadetes* was more abundant in biofilms of *V. natans* leaves, and the phyla *Patescibacteria* and *Acidobacteria* were found in biofilms of *P. maackianus* leaves (Fig. S4d, e). The phyla *Patescibacteria* and *Verrucomicrobia* were significantly more abundant in biofilms of *P. maackianus* leaves than in biofilms of *V. natans* leaves, while *Armatimonadetes* showed the opposite pattern (Fig. S4f). Heatmaps with hierarchical cluster results indicated that epiphytic bacteria of three submerged macrophyte leaves in July (HJ, PJ, VJ) clustered together, epiphytic bacteria in October (HO, PO, VO) clustered together, and bacterioplankton in water in July and October (WJ, WO) clustered together (Fig. S5). Moreover, communities of epiphytic bacteria in July and October (HJ, HO, PJ, PO, VJ, and VO) clustered more closely to each other and farther from bacterioplankton in July and October (WJ, WO) (Fig. S5).

3.4. Variations in epiphytic bacterial and planktonic bacterial community

To define clearer clusters, principal coordinate analysis was applied to indicate the differences in community composition between planktonic bacteria and epiphytic bacteria as well as the differences in epiphytic bacterial community composition between the three submerged macrophytes in the two seasons. Obviously, the epiphytic bacteria of the three submerged macrophytes were completely separated from planktonic bacteria in the PCoA diagram (Fig. S6a). The result was confirmed by using ANOSIM analysis (Fig. S6b, c, d). ANOSIM also implied significant differences in epiphytic bacterial community composition between July and October (Fig. S6e). In addition, the PCoA and ANOSIM analysis showed that there were significant differences in epiphytic bacterial community composition among the three submerged macrophytes in the two seasons ($P < 0.05$) (Fig. 5, S6f and g). An LEfSe analysis was used to analyze the distribution of differences in the epiphytic bacterial taxa between the three submerged macrophytes in more detail from the phylum to genus levels (Fig. 6). The graph was based on LDA scores >3.5 ($P < 0.05$). At the genus level, nine different indicator genera were present in epiphytic bacteria of the three submerged macrophytes. *Romboutsia*, *Methylophilus* and *Methylotenera* were increased significantly in the biofilm attached to *H. verticillate*. *Nostoc_PCC_8976*, *Calothrix_KVSF5*, *Leptolyngbya_PCC_6406* and *Acidibacter* were increased significantly in the biofilm attached to *P. maackianus*. *Phyllobacterium* and *Methyloglobulus* were increased significantly in the biofilm attached to *V. natans* (Fig. 6).

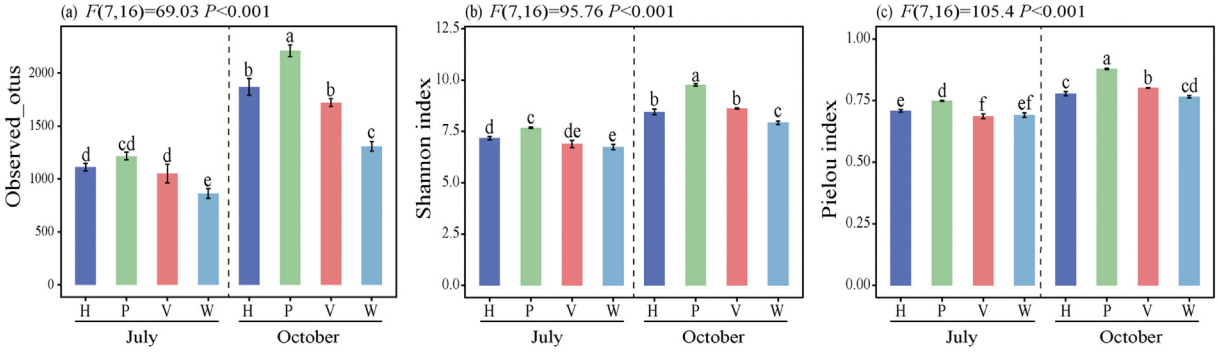

Fig. 3. Alpha diversity estimates of epiphytic bacteria on three submerged macrophytes and bacterioplankton in water in July and October. (a) OTU richness estimates (number of observed OTUs), (b) Shannon diversity indices and (c) Pielou's evenness estimates. H, biofilm of *H. verticillata*; P, biofilm of *P. maackianus*; V, biofilm of *V. natans*; W, water. Different letters (a, b, c, d, e, f) represent significant differences ($P < 0.05$) in mean value by means of one-way ANOVAs and LSD post-hoc comparisons.

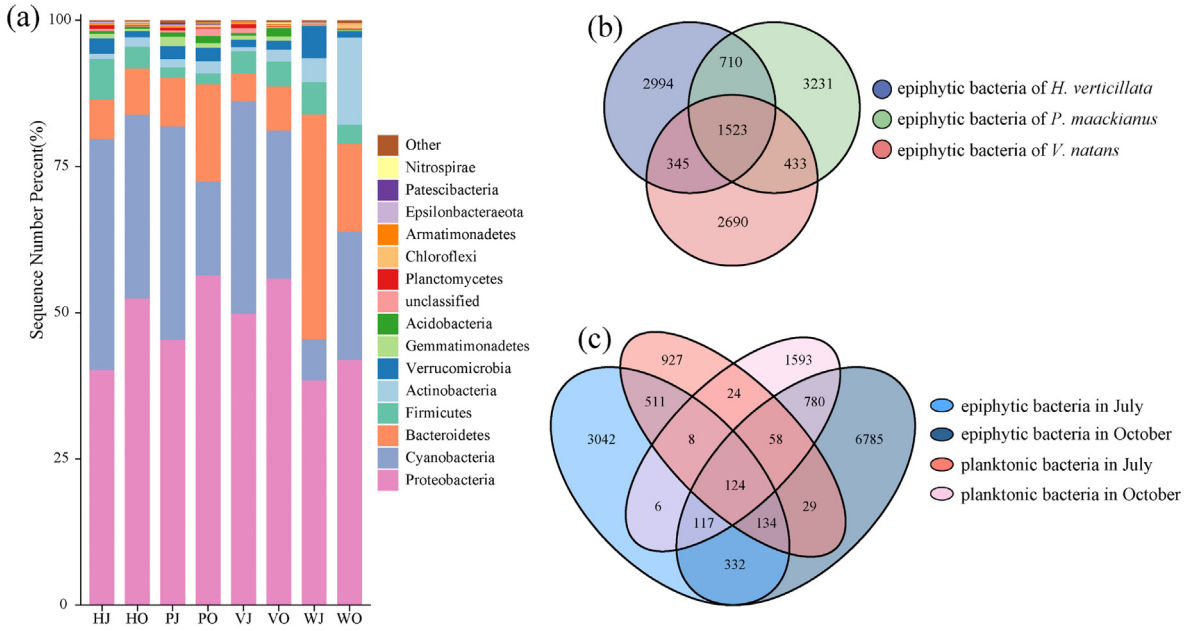

Fig. 4. Community compositions of bacteria (top 15) at the phylum level across different groups in July and October (a). Venn diagram based on OTUs of the epiphytic bacteria among the three submerged macrophytes (b). Venn diagram based on OTUs of epiphytic bacteria and planktonic bacteria in July and October (c). HJ, biofilm of *H. verticillata* in July; HO, biofilm of *H. verticillata* in October; PJ, biofilm of *P. maackianus* in July; PO, biofilm of *P. maackianus* in October; VJ, biofilm of *V. natans* in July; VO, biofilm of *V. natans* in October; WJ, water in July; WO, water in October.

3.5. Prediction of microbial functions

To explore the role of bacterial communities in energy metabolism, we used PICRUSt2 to perform a functional prediction analysis of the 16S sequences and a comparative analysis of the predicted functions at the energy metabolism level of the third KEGG pathway. PICRUSt2 analysis indicated that the functional gene families were carbon fixation, photosynthesis, nitrogen metabolism, oxidative phosphorylation, sulfur metabolism and methane metabolism (Fig. 7a). Compared with the epiphytic bacteria, the abundance of oxidative phosphorylation and carbon fixation in photosynthetic organisms was significantly higher ($P < 0.05$) in the planktonic bacteria (Fig. 7b). In addition, the functional genes of carbon fixation, nitrogen metabolism, oxidative phosphorylation, sulfur metabolism and methane metabolism of epiphytic bacteria were significantly more abundant in October than in July ($P < 0.05$), while photosynthesis showed the opposite pattern (Fig. 7c). In July, the functional genes of nitrogen metabolism, methane metabolism, sulfur metabolism and carbon fixation pathways in prokaryotes of epiphytic bacteria were significantly more abundant in *V. natans* than in *H. verticillata* ($P < 0.05$), while photosynthesis showed the opposite pattern (Fig. S7a). The functional genes of nitrogen metabolism and oxidative phosphorylation of epiphytic bacteria were significantly more abundant in *P. maackianus* than in *H. verticillata* ($P < 0.05$), while carbon fixation in photosynthetic organisms showed the opposite pattern (Fig. S7b). The functional genes of nitrogen metabolism, methane metabolism, sulfur metabolism and carbon fixation pathways in prokaryotes of epiphytic bacteria were significantly more abundant in *V. natans* than in *P. maackianus* ($P < 0.05$), while photosynthesis and oxidative phosphorylation showed the opposite pattern (Fig. S7c). In October, the oxidative phosphorylation functional genes of epiphytic bacteria were significantly more abundant in *V. natans* and *P. maackianus* than in *H. verticillata* ($P < 0.05$) (Fig. S7d, e). The functional genes of carbon fixation, oxidative phosphorylation and nitrogen metabolism of epiphytic bacteria were significantly more abundant in *P. maackianus* than in *V. natans* ($P < 0.05$), while photosynthesis showed the opposite pattern (Fig. S7c).

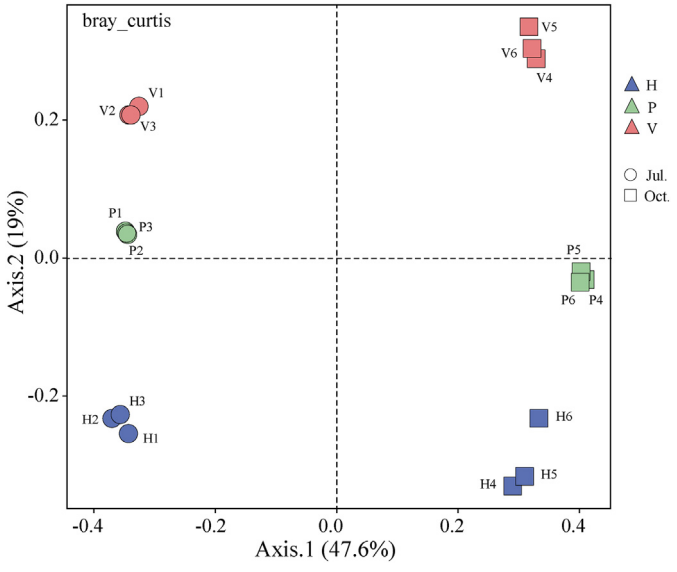

Fig. 5. Principal coordinate analysis showing the composition differences of the epiphytic bacterial community of the three submerged macrophytes at the genus level (calculated using Bray–Curtis). H, epiphytic bacteria of *H. verticillata* leaves; P, epiphytic bacteria of *P. maackianus* leaves; V, epiphytic bacteria of *V. natans* leaves.

4. Discussion

4.1. The community structure of epiphytic bacteria

In this study, *Proteobacteria* was the most dominant phylum in both the epiphytic bacterial community and planktonic bacterial community (Fig. 4a), but the abundance of *Proteobacteria* was significantly higher in the epiphytic bacterial community than in the planktonic bacterial community (Fig. S4a). Previous studies have shown that distinct and shared microorganisms exist between epiphytic and planktonic bacterial communities (Burke et al., 2011; Aguilar and Sommaruga, 2020). Both in July and October, the alpha diversity of epiphytic bacteria was significantly higher than that of planktonic bacteria (Fig. 5), because submersed macrophytes

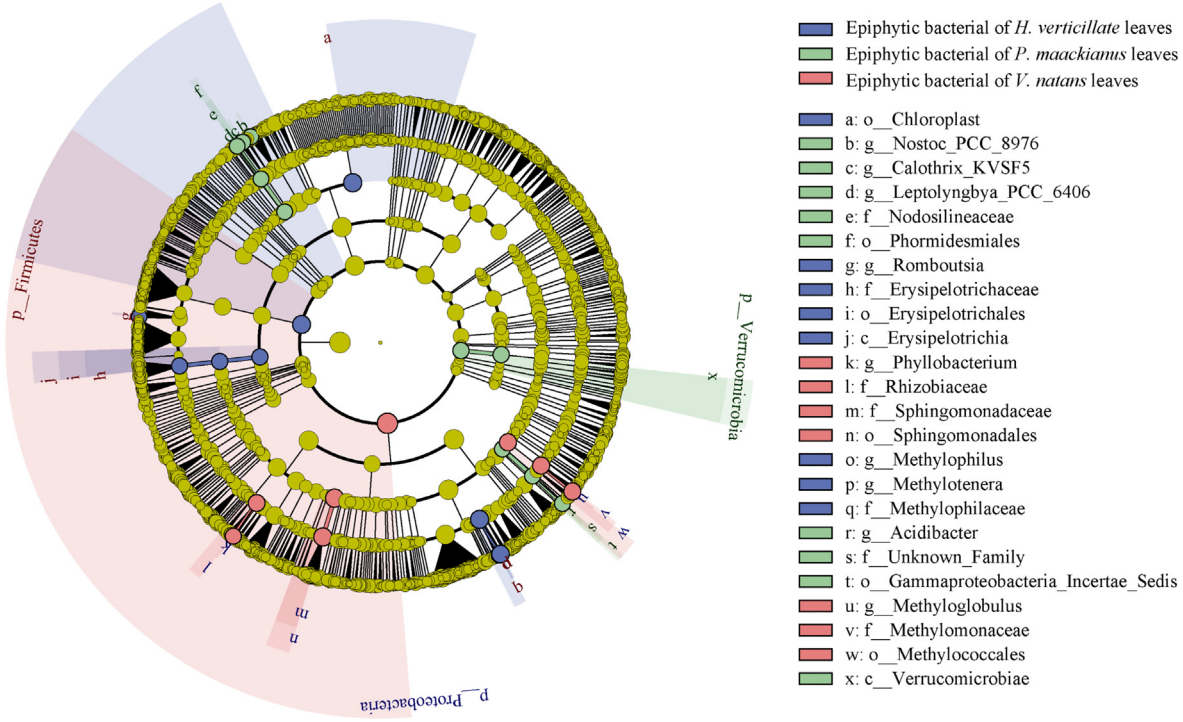

Fig. 6. Taxonomic cladogram comparing epiphytic bacterial community composition of the three submerged macrophytes by least discriminant analysis (LDA). Only the LDA score > 3.5 is shown in the figure. The innermost circle represents the phylum taxonomy level, and the outer circle in turn represents the taxonomy level of class, order, family, and genus. The size of the node represents the abundance, significantly discriminant taxon nodes are colored, and the branch areas are shaded according to the highest ranked group for that taxon. When the taxon was not significantly different among the sample groups, the corresponding node was colored yellow.

can provide nutrients and release allelopathic substances to epiphytic microbes, increasing the richness and diversity of bacterial communities (He et al., 2012; Liu et al., 2020). Moreover, the beta diversity of the epiphytic bacterial community was different from that of the planktonic bacterial community (Fig. S6). This result may be caused by the effects of selection and biofilm physicochemical properties of submerged macrophytes on the epiphytic bacterial community (Chase and Myers, 2011; Dini-Andreote et al., 2015).

The growing season was an important factor that affected the community structure of epiphytic bacteria on submerged macrophytes (Salmaso et al., 2018; Sun et al., 2021). Clear seasonal patterns were observed in the epiphytic bacteria on the three submerged macrophytes in our study. On the biofilms of the three submerged macrophytes, the alpha diversity of epiphytic bacteria was significantly higher in October than in July (Fig. 3), and their epiphytic bacterial compositions were also significantly different (Fig. 5, S6e). On the one hand, this is due to the influence of temperature. For example, community diversity and richness increased from July to November, and temperature was the most important driving factor for predicting seasonal changes in epiphytic bacterial community structure (Shi et al.,2022). On the other hand, the seasonal patterns of the epiphytic bacterial community might be linked with the host-plant life cycle, leaf morphology, and the surrounding water characteristics (Vokou et al., 2019; Korlevic et al., 2021). July is the macrophyte growth period in our study area, while October is the macrophyte senesce period. Moreover, the secretions and secondary metabolites of aquatic plants can inhibit epiphytic bacteria (Cai et al., 2016), while the secretions and secondary metabolites of aquatic plants are more abundant in the growing season (Grutters et al., 2016). Previous studies suggested that the growing season could affect the community structure of epiphytic bacteria through the exudation of nutrients and the production of secondary metabolites (Ponisio et al., 2019; He et al., 2021; Ma et al., 2021).

Host plants may also affect the community structure of epiphytic bacteria attached to submerged macrophytes (Zhen et al., 2020; Wijewardene et al., 2022). In this study, *Proteobacteria*, *Cyanobacteria* and *Bacteroidetes* were the dominant epiphytic bacterial phyla in the biofilms attached to the three submerged macrophyte leaves (Fig. 4a), but the abundances of the dominant epiphytic bacterial phyla were different between the three submerged macrophytes (Fig. S4d, e, f). The alpha diversity of the epiphytic bacteria in the three submerged macrophytes also differed, and the highest alpha diversity was found in the epiphytic bacteria of *P. maackianus* (Fig. 3). The higher alpha diversity in the epiphytic bacteria of *P. maackianus* might be because the DW, C, N and P were higher in the biofilm of *P. maackianus* leaves, which could provide nutrients to a wider variety of bacterial types (Zhang et al., 2020). Moreover, the PCOA and ANOSIM analysis indicated that the epiphytic bacterial compositions were significantly different at the genus level among the epiphytic bacteria on the three submerged macrophytes in the two seasons (Fig. 5, S6f and g). Furthermore, the LEfSe analysis showed the different distributions of the epiphytic bacterial taxa between the three submerged macrophytes in more detail from the phylum to genus levels (Fig. 6). These results implied that the epiphytic bacterial community among the three submerged macrophytes did differ obviously, and some specific taxa were enriched on the biofilms of the three plants. Previous studies have shown that deterministic processes and stochastic processes play basic roles in the assembly and succession of bacterial communities (Stegen et al., 2013). Dispersal and physical barriers can serve as additional factors affecting community assemblages (Burke et al., 2011; Xie et al., 2017). The different physicochemical traits of host plants could result in host-specific epiphytic bacteria (Hempel et al., 2009; Lachnit et al., 2011).

4.2. The functions of epiphytic bacteria in energy metabolism

PICRUSt2 analysis indicated that the functional gene families were carbon fixation, photosynthesis, nitrogen metabolism, oxidative phosphorylation, sulfur metabolism and methane metabolism (Fig. 7a). Photosynthesis is the most important metabolic activity of submerged plants, and has a

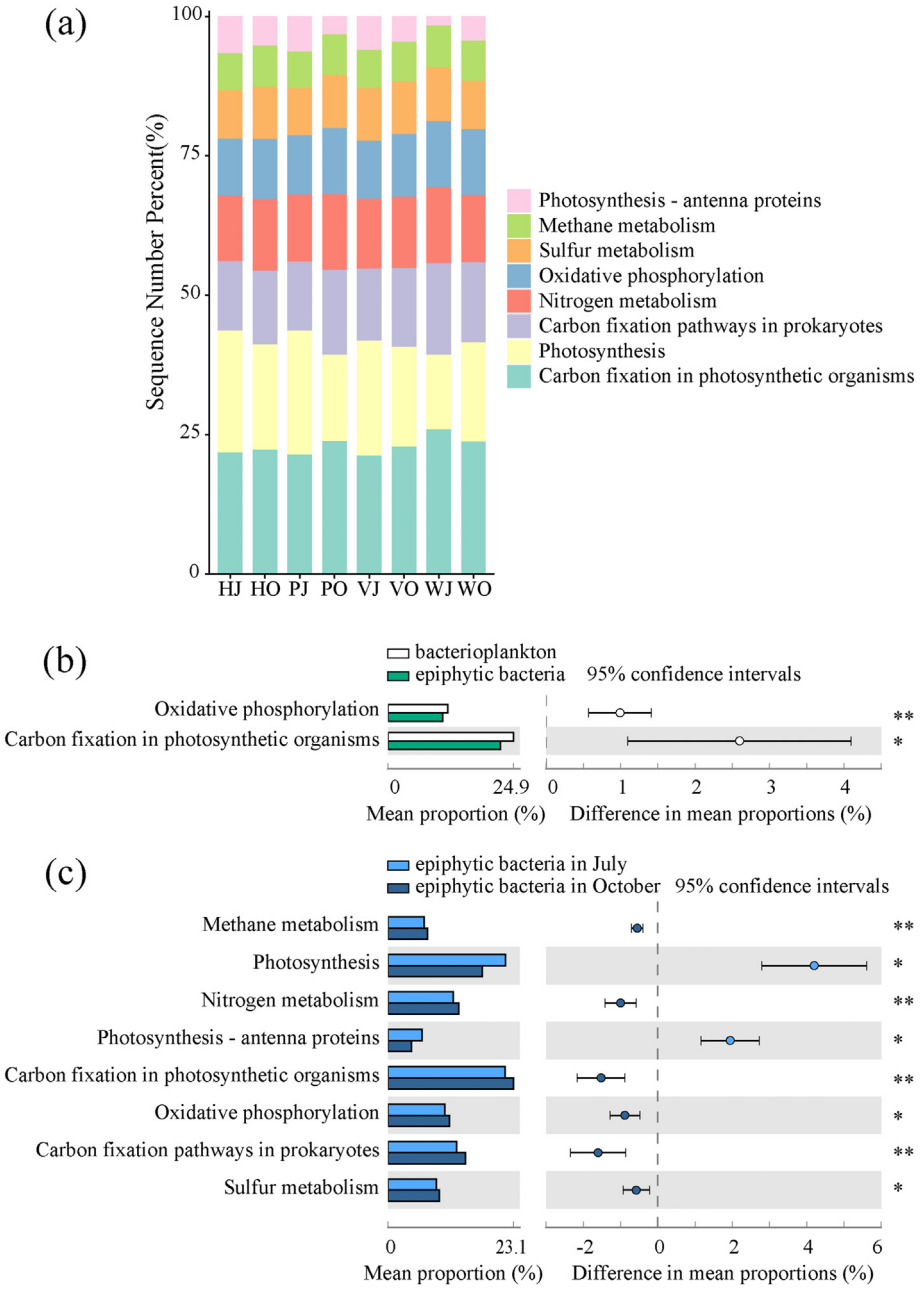

Fig. 7. The bar chart of the microbial energy metabolism functions predicted at the second KEGG pathway level in different groups across the two study periods (a). Differences in energy metabolism functions between bacterioplankton and epiphytic bacteria (b). Differences in the energy metabolism functions of epiphytic bacteria between July and October (c). Wilcoxon tests followed by Bonferroni corrections were performed. HJ, biofilm of *H. verticillata* in July; HO, biofilm of *H. verticillata* in October; PJ, biofilm of *P. maackianus* in July; PO, biofilm of *P. maackianus* in October; VJ, biofilm of *V. natans* in July; VO, biofilm of *V. natans* in October; WJ, water in July; WO, water in October.

significant impact on the structure and function of the entire aquatic ecosystem (Hunken et al., 2008; Kragh et al., 2017). The metabolism of methane is an important part of the biogeochemical cycling of carbon, while methane is also a major contributor to climate change (Evans et al., 2015; Yu and Chistoserdova, 2017). Oxidative phosphorylation constitutes the major source of ATP in aerobic organisms and includes the reactions that result in the synthesis of ATP from ADP + Pi (Wang et al., 2017; Xiao et al., 2019). Carbon, nitrogen, phosphorus and sulfur are the fundamental elements associated with the chemical composition of living organisms (Elser et al., 2007; Minden and Kleyer, 2014; Hao et al., 2017b), and their metabolism is the main form of the material cycle in lake ecosystems (Newton et al., 2011; Schauer et al., 2014), while microorganisms are an important component of lake ecosystems and the main driver of the lake material cycle (Buchan et al., 2014; Linz et al., 2018). Our study indicated that epiphytic bacteria and planktonic bacteria have important functions in plant growth and biogeochemical cycles in aquatic ecosystems. Moreover, the abundance of functional genes exhibited significant differences between planktonic and epiphytic bacteria in the two growth seasons, as well as among epiphytic bacteria attached to the three submerged macrophytes (Fig. 7b, c) (Fig. S7). The functions of microorganisms might be determined by their compositions. A previous study found that the phylum *Proteobacteria* and the classes *Betaproteobacteria* and *Gammaproteobacteria* are involved in the degradation of organic matter in sewage treatment systems and the reduction of nitrate and nitrite (Cheng et al., 2016). Therefore, the results might be caused by the different compositions of dominant taxa in planktonic and epiphytic bacterial communities in the two seasons.

Among the three submerged macrophytes, the abundance of functions related to nitrogen and phosphorus transformation was higher in the epiphytic bacteria of *P. maackianus* (Fig. S7). These differences might be related to the different physicochemical properties (DW, BTN and BTP) in the biofilm of *P. maackianus* (Zhang et al., 2020; Wang et al., 2021a). Therefore, the species *P. maackianus* might play more important roles in the recovery of eutrophic lakes in the middle and lower reaches of the Yangtze River.

5. Conclusion

In this study, we found that the community compositions and functions of epiphytic bacterial communities on submerged macrophyte hosts were different from those of the planktonic bacterial communities in the surrounding water. The growth season of submerged macrophytes had great influences on the structure and functions of the epiphytic bacterial community. The structure and functions of the epiphytic bacterial community exhibited obvious differences among the three submerged macrophytes, and some specific taxa were enriched in the biofilms of the three different plants. In addition, epiphytic bacteria have important functions in plant growth and regulating the migration and transformation of nutrients (contaminants) in aquatic ecosystems. Overall, this study provided clues for understanding the distribution and formation mechanisms of epiphytic bacteria on submerged macrophyte leaves and their roles in freshwater ecosystems.

CRediT authorship contribution statement

Weicheng Yu collected and analyzed the data and wrote the manuscript. Jiahe Li, Xiaowen Ma, Tian Lv and Ligong Wang collected the data and contributed to the manuscript. Jiaru Li and Chunhua Liu designed the experiment, revised this manuscript and provided fund support.

Declaration of competing interest

The authors declare that they have no known competing financial interests or personal relationships that could have appeared to influence the work reported in this paper.

Acknowledgements

Special thanks to Yang Li and Chuanxin Chao for their valuable suggestions for this manuscript. The authors gratefully acknowledge funding support from the Fundamental Research Funds for the Central Universities (2042020kf1025).

Appendix A. Supplementary data

Supplementary data to this article can be found online at https://doi.org/10.1016/j.scitotenv.2022.155546.

References

Aguilar, P., Sommaruga, R., 2020. The balance between deterministic and stochastic processes in structuring lake bacterioplankton community over time. Mol. Ecol. 29, 3117–3130.

Bai, G.L., Zhang, Y., Yan, P., Yan, W.H., Kong, L.W., Wang, L., et al., 2020. Spatial and seasonal variation of water parameters, sediment properties, and submerged macrophytes after ecological restoration in a long-term (6 year) study in Hangzhou west lake in China: submerged macrophyte distribution influenced by environmental variables. Water Res. 186, 15.

Bao, S.D., 2000. Soil Agrochemical Analysis. Third edition. China Agricultural Press, Beijing.

Buchan, A., LeCleir, G.R., Gulvik, C.A., Gonzalez, J.M., 2014. Master recyclers: features and functions of bacteria associated with phytoplankton blooms. Nat. Rev. Microbiol. 12, 686–698.

Burke, C., Thomas, T., Lewis, M., Steinberg, P., Kjelleberg, S., 2011. Composition, uniqueness and variability of the epiphytic bacterial community of the green alga Ulva australis. ISME J. 5, 590–600.

Cai, X.L., Yao, L., Gao, G., Xie, Y.F., Zhang, Y.Y., Tang, X.M., 2016. The response of epiphytic bacteria on Vallisneria natans (Lour.) hara (Hydrocharitaceae) to increasing nutrient loadings. J. Basic Microbiol. 56, 608–616.

Callahan, B.J., McMurdie, P.J., Rosen, M.J., Han, A.W., Johnson, A.J.A., Holmes, S.P., 2016. DADA2: high-resolution sample inference from illumina amplicon data. Nat. Methods 13, 581.

Chae, S.S., Warde, W.D., 2006. Effect of using principal coordinates and principal components on retrieval of clusters. Comput. Stat. Data Anal. 50, 1407–1417.

Chao, C.X., Wang, L.G., Li, Y., Yan, Z.W., Liu, H.M., Yu, D., et al., 2021. Response of sediment and water microbial communities to submerged vegetations restoration in a shallow eutrophic lake. Sci. Total Environ. 801, 12.

Chase, J.M., Myers, J.A., 2011. Disentangling the importance of ecological niches from stochastic processes across scales. Philos. Trans. R. Soc. BBiol. Sci. 366, 2351–2363.

Chen, H., Boutros, P.C., 2011. Venndiagram: a package for the generation of highly-customizable Venn and Euler diagrams in R. BMC Bioinformatics 12, 7.

Cheng, C., Xie, H.J., Yang, E., Shen, X.X., Dai, P., Zhang, J., 2016. Nutrient removal and microbial mechanisms in constructed wetland microcosms treating high nitrate/nitrite polluted river water. RSC Adv. 6, 70848–70854.

Coci, M., Nicol, G.W., Pilloni, G.N., Schmid, M., Kamst-van Agterveld, M.P., Bodelier, P.L.E., et al., 2010. Quantitative assessment of ammonia-oxidizing bacterial communities in the epiphyton of submerged macrophytes in shallow lakes. Appl. Environ. Microbiol. 76, 1813–1821.

Dini-Andreote, F., Stegen, J.C., van Elsas, J.D., Salles, J.F., 2015. Disentangling mechanisms that mediate the balance between stochastic and deterministic processes in microbial succession. Proc. Natl. Acad. Sci. U. S. A. 112, E1326–E1332.

Douglas, G.M., Maffei, V.J., Zaneveld, J.R., Yurgel, S.N., Brown, J.R., Taylor, C.M., et al., 2020. PICRUSt2 for prediction of metagenome functions. Nat. Biotechnol. 38, 685–688.

Elser, J.J., Bracken, M.E.S., Cleland, E.E., Gruner, D.S., Harpole, W.S., Hillebrand, H., et al., 2007. Global analysis of nitrogen and phosphorus limitation of primary producers in freshwater, marine and terrestrial ecosystems. Ecol. Lett. 10, 1135–1142.

Evans, P.N., Parks, D.H., Chadwick, G.L., Robbins, S.J., Orphan, V.J., Golding, S.D., et al., 2015. Methane metabolism in the archaeal phylum bathyarchaeota revealed by genome-centric metagenomics. Science 350, 434–438.

Fahy, B.G., Vasilopoulos, T., Ford, S., Gravenstein, D., Enneking, F.K., 2015. A single consent for serial anesthetics in burn surgery. Anesth. Analg. 121, 219–222.

Fan, Z., Han, R.M., Ma, J., Wang, G.X., 2016. Submerged macrophytes shape the abundance and diversity of bacterial denitrifiers in bacterioplankton and epiphyton in the shallow fresh lake Taihu, China. Environ. Sci. Pollut. Res. 23, 14102–14114.

Gao, H.L., Qian, X., Wu, H.F., Li, H.M., Pan, H., Han, C.M., 2017. Combined effects of submerged macrophytes and aquatic animals on the restoration of a eutrophic water body-a case study of Gonghu Bay, Lake Taihu. Ecol. Eng. 102, 15–23.

Ge, Y.W., Zhang, K., Yang, X.D., 2018. Long-term succession of aquatic plants reconstructed from palynological records in a shallow freshwater lake. Sci. Total Environ. 643, 312–323.

Gordon-Bradley, N., Lymperopoulou, D.S., Williams, H.N., 2014. Differences in bacterial community structure on Hydrilla verticillata and Vallisneria americana in a freshwater spring. Microbes Environ. 29, 67–73.

Grace, K.A., Juston, J.M., Finn, D., DeBusk, W.F., Ivanoff, D., DeBusk, T.A., 2019. Substrate manipulation near the outflow of a constructed wetland reduced internal phosphorus loading from sediments and macrophytes. Ecol. Eng. 129, 71–81.

Grutters, B.M.C., Gross, E.M., Bakker, E.S., 2016. Insect herbivory on native and exotic aquatic plants: phosphorus and nitrogen drive insect growth and nutrient release. Hydrobiologia 778, 209–220.

Hamelin, S., Planas, D., Amyot, M., 2015. Spatio-temporal variations in biomass and mercury concentrations of epiphytic biofilms and their host in a large river wetland (Lake St. Pierre, Qc, Canada). Environ. Pollut. 197, 221–230.

Hao, B.B., Wu, H.P., Cao, Y., Xing, W., Jeppesen, E., Li, W., 2017a. Comparison of periphyton communities on natural and artificial macrophytes with contrasting morphological structures. Freshw. Biol. 62, 1783–1793.

Hao, Z., Gao, Y., Yang, T.T., 2017b. Seasonal variation of DOM and associated stoichiometry for freshwater ecosystem in the subtropical watershed: indicating the optimal C:N:P ratio. Ecol. Indic. 78, 37–47.

He, D., Ren, L.J., Wu, Q.L., 2012. Epiphytic bacterial communities on two common submerged macrophytes in Taihu Lake: diversity and host-specificity. Chin. J. Oceanol. Limnol. 30, 237–247.

He, D., Ren, L.J., Wu, Q.L.L., 2014. Contrasting diversity of epibiotic bacteria and surrounding bacterioplankton of a common submerged macrophyte, Potamogeton crispus, in freshwater lakes. FEMS Microbiol. Ecol. 90, 551–562.

He, D., Ren, L.J., Wu, Q.L.L., 2020. Growing season drives the compositional changes and assembly processes of epiphytic bacterial communities of two submerged macrophytes in Taihu Lake. FEMS Microbiol. Ecol. 96, 12.

He, D., Zheng, J.W., Ren, L.J., Wu, Q.L., 2021. Substrate type and plant phenolics influence epiphytic bacterial assembly during short-term succession. Sci. Total Environ. 792, 10.

Hempel, M., Grossart, H.P., Gross, E.M., 2009. Community composition of bacterial biofilms on two submerged macrophytes and an artificial substrate in a pre-alpine lake. Aquat. Microb. Ecol. 58, 79–94.

Hilt, S., Alirangues Nunez, M.M., Bakker, E.S., Blindow, I., Davidson, T.A., Gillefalk, M., et al., 2018. Response of submerged macrophyte communities to external and internal restoration measures in north temperate shallow lakes. Front. Plant Sci. 9, 24.

Horppila, J., Nurminen, L., 2003. Effects of submerged macrophytes on sediment resuspension and internal phosphorus loading in Lake Hiidenvesi (southern Finland). Water Res. 37, 4468–4474.

Hunken, M., Harder, J., Kirst, G.O., 2008. Epiphytic bacteria on the Antarctic ice diatom Amphiprora kufferathii Manguin cleave hydrogen peroxide produced during algal photosynthesis. Plant Biol. 10, 519–526.

Janssen, K., Low, S.L., Wang, Y., Mu, Q.Y., Bierbaum, G., Gee, C.T., 2021. Elucidating biofilm diversity on water lily leaves through 16S rRNA amplicon analysis: comparison of four DNA extraction kits. Appl. Plant Sci. 9, 15.

Jiang, H.Y., Li, J., Zhang, B., Huang, R., Zhang, J.H., Chen, Z.W., et al., 2019. Intestinal flora disruption and novel biomarkers associated with nasopharyngeal carcinoma. Front. Oncol. 9, 20.
Korlevic, M., Markovski, M., Zhao, Z.H., Herndl, G.J., Najdek, M., 2021. Seasonal dynamics of epiphytic microbial communities on marine macrophyte surfaces. Front. Microbiol. 12, 17.
Kozik, A.J., Nakatsu, C.H., Chun, H., Jones-Hall, Y.L., 2017. Age, sex, and TNF associated differences in the gut microbiota of mice and their impact on acute TNBS colitis. Exp. Mol. Pathol. 103, 311–319.
Kragh, T., Andersen, M.R., Sand-Jensen, K., 2017. Profound afternoon depression of ecosystem production and nighttime decline of respiration in a macrophyte-rich, shallow lake. Oecologia 185, 157–170.
Kuehn, K.A., Francoeur, S.N., Findlay, R.H., Neely, R.K., 2014. Priming in the microbial landscape: periphytic algal stimulation of litter-associated microbial decomposers. Ecology 95, 749–762.
Li, H.F., Li, Z.J., Qu, J.H., Wang, J.S., 2017. Bacterial diversity in traditional jiaozi and sourdough revealed by high-throughput sequencing of 16S rRNA amplicons. LWT-Food Sci. Technol. 81, 319–325.
Lachnit, T., et al., Meske, D., Wahl, M., Harder, T., Schmitz, R., 2011. Epibacterial community patterns on marine macroalgae are host-specific but temporally variable. Environ. Microbiol. 13 (3), 655–665.
Li, Y., He, Q.K., Ma, X.W., Wang, H.J., Liu, C.H., Yu, D., 2019. Plant traits interacting with sediment properties regulate sediment microbial composition under different aquatic DIC levels caused by rising atmospheric CO2. Plant Soil 445, 497–512.
Li, Y., Wang, L.G., Chao, C.X., Yu, H.W., Yu, D., Liu, C.H., 2021. Submerged macrophytes successfully restored a subtropical aquacultural lake by controlling its internal phosphorus loading. Environ. Pollut. 268, 12.
Linz, A.M., He, S.M., Stevens, S.L.R., Anantharaman, K., Rohwer, R.R., Malmstrom, R.R., et al., 2018. Freshwater carbon and nutrient cycles revealed through reconstructed population genomes. PeerJ 6, 24.
Liu, D.Q., Tong, C., 2017. Bacterial community diversity of traditional fermented vegetables in China. LWT-Food Sci. Technol. 86, 40–48.
Liu, Q., Liu, M.M., Zhang, Q., Bao, Y.L., Yang, N., Huo, Y.Z., et al., 2019a. Epiphytic bacterial community composition on the surface of the submerged macrophyte Myriophyllum spicatum in a low-salinity sea area of Hangzhou Bay. Oceanol. Hydrobiol. Stud. 48, 43–55.
Liu, Z.G., Li, J.Y., Wei, B.L., Huang, T., Xiao, Y.S., Peng, Z., et al., 2019b. Bacterial community and composition in Jiang-shui and Suan-cai revealed by high-throughput sequencing of 16S rRNA. Int. J. Food Microbiol. 306, 9.
Liu, Y.S., Gong, L.X., Mu, X.Y., Zhang, Z.Q., Zhou, T.T., Zhang, S.H., 2020. Characterization and co-occurrence of microbial community in epiphytic biofilms and surface sediments of wetlands with submersed macrophytes. Sci. Total Environ. 715, 10.
Lv, T., He, Q.K., Hong, Y.P., Liu, C.H., Yu, D., 2018. Effects of water quality adjusted by submerged macrophytes on the richness of the epiphytic algal community. Front. Plant Sci. 9, 1980.
Ma, J., Shi, R.J., Han, R.M., Ji, M., Xu, X.G., Wang, G.X., 2021. Community structure of epiphytic bacteria on Potamogeton pectinatus and the surrounding bacterioplankton in Hongze Lake. Mar. Freshw. Res. 72, 997–1003.
Minden, V., Kleyer, M., 2014. Internal and external regulation of plant organ stoichiometry. Plant Biol. 16, 897–907.
Newton, R.J., Jones, S.E., Eiler, A., McMahon, K.D., Bertilsson, S., 2011. A guide to the natural history of freshwater lake bacteria. Microbiol. Mol. Biol. Rev. 75, 14–49.
Pei, G.F., Wang, Q., Liu, G.X., 2015. The role of periphyton in phosphorus retention in shallow lakes with different trophic status, China. 125, 17–22.
Peng, J.N., Lu, X.R., Xie, K.L., Xu, Y.S., He, R., Guo, L., et al., 2019. Dynamic alterations in the gut microbiota of collagen-induced arthritis rats following the prolonged administration of total glucosides of paeony. Front. Cell. Infect. Microbiol. 9, 17.
Philonenko, P., Postovalov, S., 2015. A new two-sample test for choosing between log-rank and wilcoxon tests with right-censored data. J. Stat. Comput. Simul. 85, 2761–2770.
Ponisio, L.C., Valdovinos, F.S., Allhoff, K.T., Gaiarsa, M.P., Barner, A., Guimaraes, P.R., et al., 2019. A network perspective for community assembly. Front. Ecol. Evol. 7, 11.
Reynaud, Y., Ducat, C., Talarmin, A., Marcelino, I., 2020. Cartography of free-living amoebae in soil in Guadeloupe (French West Indies) using DNA metabarcoding. Pathogens 9, 13.
Salmaso, N., Albanese, D., Capelli, C., Boscaini, A., Pindo, M., Donati, C., 2018. Diversity and cyclical seasonal transitions in the bacterial community in a large and deep perialpine lake. Microb. Ecol. 76, 125–143.
Schauer, R., Risgaard-Petersen, N., Kjeldsen, K.U., Bjerg, J.J.T., Jorgensen, B.B., Schramm, A., et al., 2014. Succession of cable bacteria and electric currents in marine sediment. ISME J. 8, 1314–1322.
Schlechter, R.O., Miebach, M., Remus-Emsermann, M.N.P., 2019. Driving factors of epiphytic bacterial communities: a review. J. Adv. Res. 19, 57–65.
Srivastava, J.K., Chandra, H., Kalra, S.J.S., Mishra, P., Khan, H., Yadav, P., 2017. Plant-microbe interaction in aquatic system and their role in the management of water quality: a review. Appl Water Sci 7, 1079–1090.
Stegen, J.C., Lin, X.J., Fredrickson, J.K., Chen, X.Y., Kennedy, D.W., Murray, C.J., et al., 2013. Quantifying community assembly processes and identifying features that impose them. ISME J. 7, 2069–2079.
Sun, L., Wang, J.S., Wu, Y.Y., Gao, T.Y., Liu, C.Q., 2021. Community structure and function of epiphytic bacteria associated with Myriophyllum spicatum in Baiyangdian Lake China. Front. Microbiol. 12, 10.
Vokou, D., Genitsaris, S., Karamanoli, K., Vareli, K., Zachari, M., Voggoli, D., et al., 2019. Metagenomic characterization reveals pronounced seasonality in the diversity and structure of the phyllosphere bacterial community in a Mediterranean ecosystem. Microorganisms. 7, 19.
Wang, Q.H., Zhao, C., Zhang, M., Li, Y.Z., Shen, Y.Y., Guo, J.X., 2017. Transcriptome analysis around the onset of strawberry fruit ripening uncovers an important role of oxidative phosphorylation in ripening. Sci. Rep. 7, 11.
Wang, C., Liu, S.Y., Zhang, Y., Liu, B.Y., He, F., Xu, D., et al., 2018. Bacterial communities and their predicted functions explain the sediment nitrogen changes along with submerged macrophyte restoration. Microb. Ecol. 76, 625–636.
Wang, Y., Samaranayake, L.P., Dykes, G.A., 2021a. Plant components affect bacterial biofilms development by altering their cell surface physicochemical properties: a predictability study using actinomyces naeslundii. FEMS Microbiol. Ecol. 97, 8.
Wang, Y.T., Wang, W.C., Zhou, Z.Z., Xia, W., Zhang, Y.X., 2021b. Effect of fast restoration of aquatic vegetation on phytoplankton community after removal of purse seine culture in Huayanghe Lakes. Sci. Total Environ. 768, 10.
Webb-Robertson, B.J., Bunn, A.L., Bailey, V.L., 2011. Phospholipid fatty acid biomarkers in a freshwater periphyton community exposed to uranium: discovery by non-linear statistical learning. J. Environ. Radioact. 102, 64–71.
Wijewardene, L., Wu, N.A., Fohrer, N., Riis, T., 2022. Epiphytic biofilms in freshwater and interactions with macrophytes: current understanding and future directions. Aquat. Bot. 176, 11.
Wolters, J.W., Reitsema, R.E., Verdonschot, R.C.M., Schoelynck, J., Verdonschot, P.F.M., Meire, P., 2019. Macrophyte-specific effects on epiphyton quality and quantity and resulting effects on grazing macroinvertebrates. Freshw. Biol. 64, 1131–1142.
Wu, Y.H., 2016. Periphyton: Functions and Application in Environmental Remediation. Elsevier.
Xia, P.H., Yan, D.B., Sun, R.G., Song, X., Lin, T., Yi, Y., 2020. Community composition and correlations between bacteria and algae within epiphytic biofilms on submerged macrophytes in a plateau lake, Southwest China. Sci. Total Environ. 727, 11.
Xian, L., Wan, T., Cao, Y., Sun, J.Y., Wu, T., Apudo, A.A., et al., 2020. Structural variability and functional prediction in the epiphytic bacteria assemblies of Myriophyllum spicatum. Curr. Microbiol. 77, 3582–3594.
Xiao, C.Y., Wang, L.H., Hu, D.D., Zhou, Q., Huang, X.H., 2019. Effects of exogenous bisphenol A on the function of mitochondria in root cells of soybean (Glycine max L.) seedlings. Chemosphere 222, 619–627.
Xie, X.F., He, Z.L., Hu, X.J., Yin, H.Q., Liu, X.D., Yang, Y.F., 2017. Large-scale seaweed cultivation diverges water and sediment microbial communities in the coast of Nan'ao island, South China Sea. Sci. Total Environ. 598, 97–108.
Yan, L.Y., Zhang, S.H., Lin, D., Guo, C., Yan, L.L., Wang, S.P., et al., 2018. Nitrogen loading affects microbes, nitrifiers and denitrifiers attached to submerged macrophyte in constructed wetlands. Sci. Total Environ. 622, 121.
Yu, Z., Chistoserdova, L., 2017. Communal metabolism of methane and the rare earth element switch. J. Bacteriol. 199, 12.
Zhang, S.H., Pang, S., Wang, P.F., Wang, C., Guo, C., Addo, F.G., et al., 2016a. Responses of bacterial community structure and denitrifying bacteria in biofilm to submerged macrophytes and nitrate. Sci. Rep. 6, 10.
Zhang, Z.Q., Chen, H.Z., Mu, X.Y., Zhang, S.H., Pang, S., Ohore, O.E., 2020. Nitrate application decreased microbial biodiversity but stimulated denitrifiers in epiphytic biofilms on Ceratophyllum demersum. J. Environ. Manag. 269, 10.
Zhao, Z.H., Qin, Z.R., Xia, L.L., Zhang, D., Mela, S.M., Li, Y., 2019. The responding and ecological contribution of biofilm-leaves of submerged macrophytes on phenanthrene dissipation in sediments. Environ. Pollut. 246, 357–365.
Zhen, Z., Yan, C.Z., Zhao, Y., 2020. Epiphytic bacterial community enhances arsenic uptake and reduction by Myriophyllum verticillatum. Environ. Sci. Pollut. Res. 27, 44205–44217.